IEEE Access
Multidisciplinary | Rapid Review | Open Access Journal

Received December 16, 2021, accepted December 31, 2021, date of publication January 6, 2022, date of current version January 18, 2022.

Digital Object Identifier 10.1109/ACCESS.2022.3140928

AC Breakdown Voltage and Partial Discharge Activity in Synthetic Ester-Based Fullerene and Graphene Nanofluids

HOCINE KHELIFA, (Member, IEEE), ERIC VAGNON, (Member, IEEE), AND ABDERRAHMANE BEROUAL, (Fellow, IEEE)
University of Lyon, Ecole Centrale de Lyon, Ampère CNRS UMR5005, 69130 Ecully, France
Corresponding author: Hocine Khelifa (hocine.khelifa@ec-lyon.fr)

ABSTRACT This paper deals with the study of the AC breakdown voltage (BDV) and partial discharges (PDs) activity of synthetic ester-based nanofluids (NF) with two kinds of carbonic nanoparticles (NPs), namely graphene (Gr) and fullerene (C_{60}); the synthetic ester (SE) being Midel 7131. The BDV measurement was achieved at various concentrations of NPs and different electrodes gap distances, while the partial discharges activity was studied only at the optimal concentration that gave the best improvements of BDV. First, a detailed improved procedure for preparing our NFs is presented. Then, the zeta potential measurements are performed on these NFs, and their stability is checked. After the preparation and characterization of samples, the BDVs and PDs parameters are measured according to IEC 60156 (modified gap distance) and IEC 60270 standards, respectively. Finally, conformity of the experimental data with Normal and Weibull distributions is examined, and the BDV at cumulative probabilities of 1% and 50% are then deduced. It is shown that BDV outcomes for all studied liquids obey both Normal and Weibull distributions, and the BDVs at cumulative probabilities of 1% and 50% are improved. Moreover, adding Gr and C_{60} nanoparticles at different concentrations enhances the BDV values for investigated electrode gaps (0.1 to 2.0mm). The best improvement is obtained with a concentration of 0.4 g/L for 0.5mm and 0.7mm electrode gap with fullerene and Graphene nanoparticles, respectively. For a 2mm gap distance, the best improvements are of about 12.67% and 16.64% with 0.4g/L of C_{60} and 0.3 g/L of Gr, respectively. It is also shown that the addition of C_{60} significantly reduces the activity of partial discharges compared to pure SE, while the addition of Gr destroys the partial discharges resistance of pure SE.

INDEX TERMS Nanofluids, synthetic ester, graphene, fullerene, AC breakdown voltage, statistical analysis, normal distribution, Weibull distribution, partial discharges.

I. INTRODUCTION

The concept of fluids mixed with nanoscale particles (called nanofluids) was first proposed by Choi and Eastman [1] in 1995 for their use in equipment/systems where cooling is required. They found indeed that this kind of fluid has better thermal conductivity, thermal diffusivity and convective heat transfer coefficient than the base fluid. Since then, much work has been engaged in the development of nanofluids and the analysis of the other properties they can have. So, it has been reported that the addition of some specific nanoparticles allows to improve significantly the dielectric properties of liquid insulators [2]–[9]. The heat transfer and insulating properties are two fundamental properties required for some applications such high voltage power transformers.

In the present work, we are more particularly interested in the insulating properties of nanofluids. Various types of nanoparticles (conducting, semi-conducting and insulating) and insulating liquids (mineral oils, synthetic and natural esters) have been investigated. So, it has been reported that synthetic ester (SE)-based nanofluids (NFs) with iron oxide (Fe_3O_4), aluminum oxide (Al_2O_3), and silicon dioxide (SiO_2) nanoparticles (NPs) show a better AC breakdown voltage (AC BDV) compared to pure SE [4], [10]. Duzkaya et Beroual [6] showed that natural ester (NE)-based NFs with semi-conductive NPs (zinc-oxide, ZnO) can improve the AC BDV by about 5%. This enhancement is obtained with a concentration of 0.1 g/L. In the case of mineral

The associate editor coordinating the review of this manuscript and approving it for publication was Nagarajan Raghavan.

oil, the enhancement reaches 75% of AC BDV with Al_2O_3 NPs at a concentration of 0.05 g/L [11]. They observed a correlation between the size of NPs and dielectric strength; the smallest NPs give the best improvement on AC BDV. Hussain *et al.* [12] studied the effect of the addition of three NPs (iron oxide "Fe_3O_4", cobalt oxide "Co_3O_4", and iron phosphide "Fe_3P") on the insulation performances of synthetic ester and natural ester (NE)-based nanofluids. All the NFs show enhancements in the dielectric strength. The optimal improvements were achieved with Fe_3P NFs (SE and NE) at a concentration of 0.002wt.% (0.02g/L). Those enhancement are 20.2 and 31.4%, for SE and NE-based NFs, respectively. Khaled and Beroual [13] reported experimental results concerning conductive NPs (Fe_3O_4) at various concentrations on the dielectric strength of mineral oil, synthetic and natural esters. The AC BDV was doubled with mineral oil-based NFs and enhanced by about 48% with SE-based NFs at a concentration of 0.4 g/L. While with NE-based NFs, the addition of Fe_3O_4 had no significant influence on the insulation performance; the improvement did not exceed 7%. Furthermore, Sima *et al.* [14] investigated the possible implication of the conductivity and permittivity of three NPs of metal oxides on the transformer oil performances. Ionization models of transformer oil-based NFs were developed. This model indicates that NPs whose conductivity or permittivity is not equal to that of the base liquid have increased saturation charges on their interface, which significantly affects/slows down the evolution of the streamers by enhancing the dielectric strength of NFs.

Besides AC breakdown voltage investigations and the possible mechanisms, partial discharges (PDs) of NFs is still little considered. Jin *et al.* [15], [16] compared the PDs activity in mineral oil with mineral oil-based NFs with fullerene and silica NPs at 0.01wt.%. It showed that the inception voltage was enhanced by about 20% with silica and by about 10% with fullerene. They assumed that the hydrophilic behavior of silica NFs can reduce the moisture content, hence enhancing the PD resistivity. Also, the discharge magnitudes of NFs were reduced by about 60% with silica and 36% with C_{60} compared to pure mineral oil. Atiya *et al.* [17] compared mineral oil-based NFs with alumina (Al_2O_3) impregned pressboard (NFs impregned pressboard, NIP) (with mineral oil impregned pressboard (M-OIP) in terms of PD activity. They reported that NIP manifests higher inception voltages than M-OIP. Furthermore, at different applied voltages, they observed that the addition of NPs reduces the generation rate of PDs pulses. The PDs current was also reduced in case of NIP at positive and negative polarity. The same authors investigated the effect of the type and the size of NPs; they were the first to propose that the electrical double layer (EDL) around NPs could affect the PDs activity [18]. They concluded that the larger the NP are, the more resistant to the activity of PDs is. Imani *et al.* [19] showed that PDs tend to be initiated predominantly at positive half-cycle by increasing the concentration of conductive NPs (Fe_3O_4), unlike pure liquid, which mainly appears at negative half-cycle. According to them, this alternation could be due to the electrohydrodynamic behavior of Fe_3O_4 NF and to the orientation of the magnetizable magnetic NPs under sinusoidal voltage.

It appears from the reported results that the commonly investigated NPs for preparing NFs are metals-oxide (iron-oxide, titanium-oxide, aluminum-oxide, ...) [5], [6], [14], [20]–[25]. In contrast, carbon nanomaterials are less investigated [3], [15], [26]–[28]. Carbon nanomaterials or Nanocarbon (NC) is a growing field of interest for designing new materials/apparatus with superior properties/performances [29]–[32]. The word 'nanocarbon' is extensively used to refer to the family of nanoscale-based carbon integrators whose properties depend mainly on the type and the three-dimensional patterns of carbon atoms [29], [31], [33]. There are several forms of these carbonic nanomaterials, among which fullerene, carbon nanotubes, graphene, and diamond nanoparticles (NPs) [29], [31], [34]–[36]. These nanosized materials have enormous implications for medicine, drug delivery, environment, chemistry, and energy [31], [32], [34], [35], [37]. For example, fullerene (C_{60}) and graphene (Gr) have been successfully used in the fields of sensors [38], [39], hydrogen generation [40]–[42], renewable energy [43], [44], and recently, insulation liquid-based carbon nanomaterials [2], [3], [26]. Dhar *et al.* [26] reported that graphene NPs enhance the dielectric breakdown voltage of transformer oil. This enhancement can reach 45% at a minimal concentration of 0.0075wt.% (0.075g/L). The nanostructures scavenging of the electrons from the electrically stressed oils has been proposed as the possible mechanism for delaying the streamer development and enhancing the breakdown voltage [3]. The considered paper puts forward a mathematical model to predict the nanostructures quantity of electrons trapped based on this assumption.

The present work aims to study the effect of two carbonic NPs, namely, fullerene (C_{60}) and graphene (Gr) on the performances of synthetic ester (SE)-based nanofluids with respect to the AC breakdown voltage and PDs activity. The AC breakdown voltage (AC-BDV) of SE is compared to those nanofluids at different concentrations and electrodes gap distances in a sphere-sphere configuration. PDs activity at optimal concentrations is considered. First, section two presents the procedure for preparing and characterizing nanofluids samples, the BDV and PD measurements methodology. Then, in section three, the results of BDV tests are presented, and the conformity with Weibull and normal distribution laws is carried out for one specific gap distance; the results of PDs tests according to IEC 60270 are also presented. Finally, section four discusses the results and the possible physicochemical processes implicated in BDV and PDs activity.

II. EXPERIMENTAL SETUP

A. SAMPLE'S PREPARATION

The base liquid used in this study is synthetic ester MIDEL 7131 transformer oil supplied by M&I Materials, UK; the

TABLE 1. Physicochemical properties of synthetic ester, midel 7131.

Property	MIDEL 7131
Density at 20 (°C)	0.97
Kinematic Viscosity (mm^2/sec)	
at 40 °C	29
at – 20 °C	1440
Pour point (°C)	–56
Flash point (°C)	260
Fire point (°C)	316
Water content (ppm)	50
AC BDV "60Hz" (kV)	>75
Power Factor at 90°C	< 0.008
DC Resistivity at 90°C (GΩ.m)	> 20

TABLE 2. The average diameter/thickness and density of nanoparticle/nanomaterial.

NPs	Fullerene (C_{60})	Graphene (Gr)
Size	4 – 8 nm	<15 µm
Thickness (nm)	–	11 – 15
Density (g/cm^3)	3.4	0.8 – 1.8

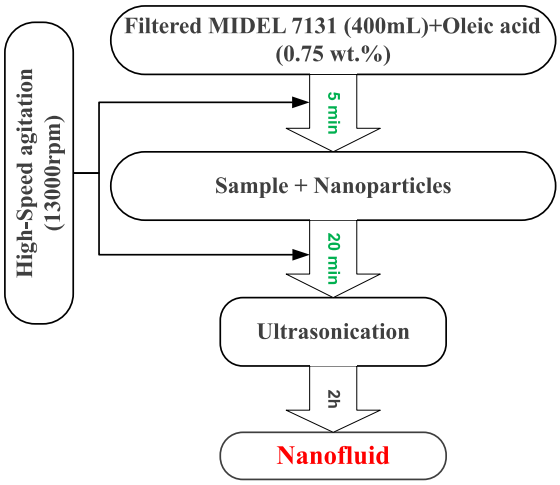

FIGURE 1. Preparation procedure of nanofluids.

physicochemical properties of this fluid are shown in Table 1. Graphene (Gr), and fullerene (C_{60}) nanoparticles with a purity of 99.5% are supplied by SkySpring Nanomaterials and Sigma-Aldrich, respectively. The fullerene NPs are spherical, while those of graphene are lamellar NPs. The average diameters of C_{60} and Gr, the thickness of Gr, the density of C_{60} and Gr NPs are given in Table 2.

Two main methods for preparing nanofluids were reported. The first one consists of combining nanoparticles synthesis and NFs preparation in a single step (one-step method), where nanoparticles are directly prepared by physical vapor deposition or a liquid chemical method. In this method, the drying, storage, transport, and dispersion processes of NPs are avoided [45]. Hence, NPs agglomeration is minimized, and fluid stability is increased. However, the downside of this method is the limited volume of the prepared NFs, which constrains its range of applications. That has been the method of choice used so far, before the recent shift to the two-step method. The second method proposes a two-step technique to prepare NFs. In the first processing step, nanoparticles, nanofibers, or nanotubes are produced as a dry powder by suitable techniques [2], [45]. Then, the nanosized powder is dispersed in the fluid. This stepwise method isolates the synthesis of NPs from the preparation of NFs [45]. As a result, agglomeration could occur in both steps, especially during NPs drying, storing, and transporting. This method is problematic as agglomeration leads to the fall of clusters under gravity, decreases thermal conductivity, and affects the dielectric properties. To address this issue, some techniques such as ultrasonic agitation (treatment) and the addition of surfactants to the fluids are often used to minimize particle aggregation and improve dispersion behavior.

In this work, the two-step method has been employed to prepare the nanofluid samples. As well as being simple, the method is practical and thus suitable for our lab-scale needs (volume and stability). The preparation steps for NFs are shown in Figure 1. The synthetic ester is first purified (removal of impurities) using a micro membrane filter and a vacuum pump. Oleic acid (supplied by Sigma-Aldrich) is then added with a mass ratio to Ester of 0.75wt.%. The assessment of the optimal mass ratio will be presented in the following section. The mixture is stirred for five minutes using the high-speed rotor-stator disperser (Misceo "250 F", 400W, 13000 rpm, and shear rate of 20m/s) at room temperature to mix the solution. Therefore, the NFs are prepared by dispersing the nanoparticles at concentrations ranging from 0.1 to 0.5 g / L (0.01 to 0.05wt.%). The NFs then undergo stirring for 20 minutes with the disperser to better disperse the nanoparticles in the ester. Subsequently, the samples of NFs are subjected to an ultrasound process for two hours to avoid agglomeration and sedimentation caused by attractive/repulsive forces. The ultrasound device (500W, 20kHz, 25mm low-intensity solid probe) operates in pulsed mode ([10s 5s], i.e., 10 sec of operation and 5 sec of rest).

B. OLEIC ACID OPTIMAL CONCENTRATION

To assess the effect of the oleic acid (OA) concentration on the NFs stability and determine the suitable concentration added to the samples, zeta potential is measured and compared for different OA concentrations ranging from 0.1 to 1.0wt.%. Five concentrations of NPs ranging from 0.1 to 0.5 g/L are investigated. However, because of the material limitation, only three concentrations of NPs (namely, 0.1; 0.2, and 0.3 g/L) are analyzed in the long-term stability. This limitation, defined as the maximum concentration needed for zeta potential measurements (0.3g/L for C_{60} and 0.2g/L for Gr), was fairly described in Malvern's user manual, which depends on the optical properties and the size of particles [46]. Therefore, a simple and efficient way to check test feasibility is by measuring absorbance value before performing zeta potential measurement. For absorbance values less

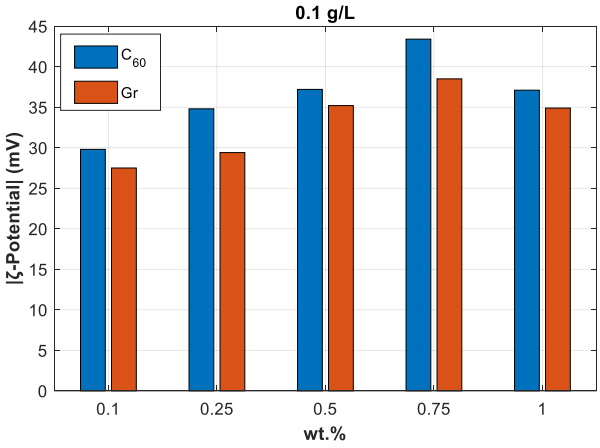

FIGURE 2. The absolute value of zeta potential evolution versus oleic acid concentration of NFs with C_{60} and Gr at the concentration of 0.1 g/L.

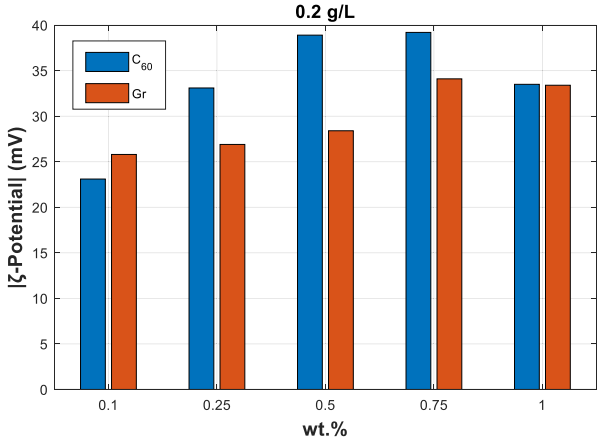

FIGURE 3. The absolute value of zeta potential evolution versus oleic acid concentration of NFs with C_{60} and Gr at the concentration of 0.2 g/L.

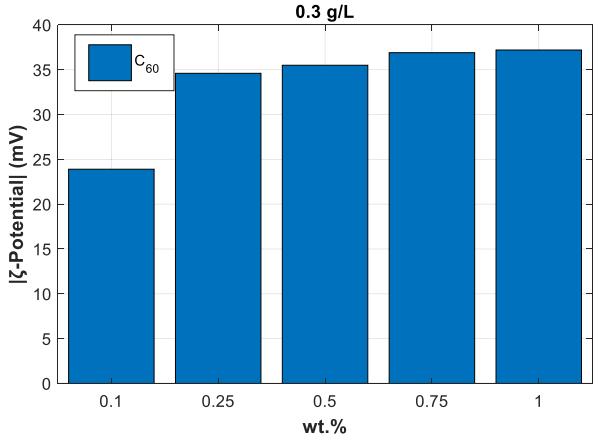

FIGURE 4. The absolute value of zeta potential evolution versus oleic acid concentration of NF with C_{60} at the concentration of 0.3 g/L.

than 100, zeta potential test will be accurate and conclusive, else the measurement will not be considered.

Figures 2 – 4 show the absolute value of zeta potential evolution versus OA concentration, considering different NFs with the different types and concentrations of NPs. Those figures show that for most cases, 0.75 wt. % of OA appear as the best compromise of concentration. Since, beyond specific surfactant concentration, the extra quantity of surface agent could form what is called micelles. This concentration called the critical micellar concentration or CMC that must be avoided, as the surface tension does not reduce further above the CMC [47].

C. CHARACTERIZATION AND STABILITY EVALUATION OF NANOFLUID

After preparing the nanofluids (NFs), the following action is to characterize them and determine their long-term stability. This is important due to the correlation between the stability of these liquids and the desired properties. Several works have shown that heat transfer properties are closely related to its stability and, even more than that, its insulating properties [48]–[50]. Therefore, particular attention was attached to this step. Several technics for the stability evaluation have been used and proven to be effective [45], including (i) sedimentation and centrifugation techniques, (ii) Zeta potential (ζ) analysis, and (iii) Spectral absorbance analysis. The hydrodynamic diameter of fullerene NPs and Zeta Potential (ζ-potential), as well as the electrical conductivity of the NFs samples, were determined thrice on a Zetasizer Nano (NS) instrument (Malvern, UK). The measurement of hydrodynamic diameter gives the first indication about the dispersion behavior of colloids and inquiry the presence of some or many clusters in the sample. Figure 5 shows the size distribution of C_{60} in MIDEL 7131 for a specified concentration (0.1 g/L). We note that the fullerene distribution presents an average size higher than the declared by the supplier (4 – 8nm). The observed difference is may be due to the fact that the NPs are coated with oleic acid, which increases their average size. Unlike C_{60} NPs which are spherical, the Gr NPs are lamellar (non-spherical). Since hydrodynamic diameter measurements are not suited using Dynamic Light Scattering Analysis (DLS-A) technique in the case of non-spherical particles. Other techniques can be used with these particles to produce high-quality images, such as Transmission electron microscopy (TEM) and Scanning Electron Microscopy (SEM) [14], [51]. Still, those techniques are not recommended for applications that need checking the long-term stability of many samples. So, zeta potential measurement appears to be the most proper technic for applications that need effective and rapid conclusions about long-term stability. The ζ-potential and electrical conductivity were measured one week after preparation; a summary of the results is given in Table 3. ζ-potential value is a chief sign of colloid stability. It intimates the potential difference between particle surface, covered with opposite and rigidly attached ions, and the neutrality point [47]. It is known that absolute zeta potential values between 0 and 10mV indicate an unstable colloid, and a surface modification or other appropriate action is needed, while if the value is between 10 and 30mV, the NFs are stable; beyond 30mV, the nanofluids become

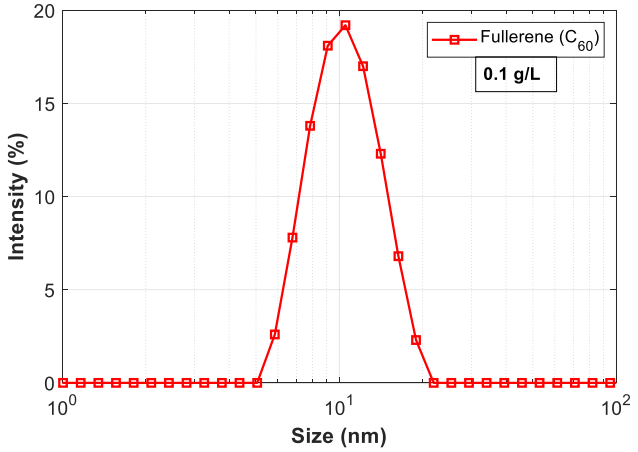

FIGURE 5. Fullerene size distribution.

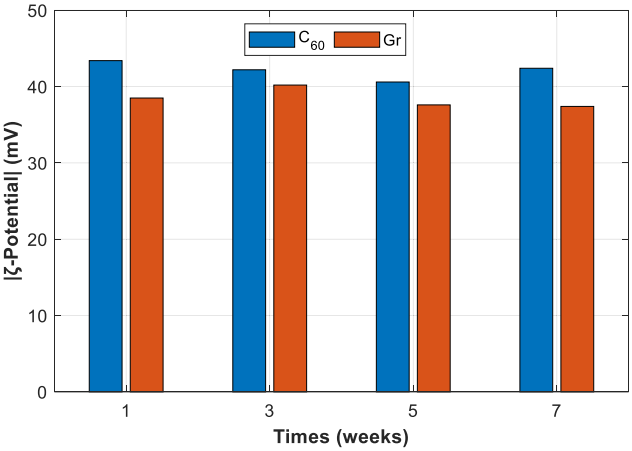

FIGURE 6. The absolute value of zeta potential of synthetic ester-based nanofluid with fullerene and graphene with a concentration of 0.1 g/L over time.

TABLE 3. Zeta potential and electrical conductivity of nanofluids samples measured after one week.

		Zeta Potential (mV)	Elec. Conductivity (mS/cm) *10^{-3}
0.1 (g/L)	C_{60}	–43.4	1.72
	Gr	–38.5	2.09
0.2 (g/L)	C_{60}	–39.2	2.98
	Gr	–34.1	3.26
0.3 (g/L)	C_{60}	–36.9	4.68
	Gr	–	–

highly stable [52]. Hence, our values indicate that our NFs are highly stable.

Nevertheless, it was observed that the absolute value of ζ-potential decreases when increasing the concentration. We could speculate that this could be due to the increased surface area or the reduced quantity of light scattered by particles. Unlike the zeta potential value, the electrical conductivity increases with the concentration because Gr and C_{60} are excellent conductors materials [29], [36]. Additionally, the electrical conductivity of SE-based NFs with Gr was higher than that with C_{60} for the same concentration, depicted in Table 3. According to the literature, this behavior may be due to the fact that Gr conducts more than C_{60} [29]. With its flat surface, the graphene nanomaterial poses a slight resistance to the crossing electrons, meaning the material has exceptionally high electron mobility result in high conductivity.

In addition to zeta potential and electrical conductivity values measured one week after the sample preparation, zeta potential evolution over time seems interesting as a stability criterion. Figure 6 shows the absolute value of zeta potential measurements of SE-based C_{60} and Gr nanofluids over seven weeks at a concentration of 0.1 g/L. It is observed that the zeta potential shows no obvious signs of decay, and all values are above the lower limit of 30mV, which indicates that our NFs are highly stable.

D. BREAKDOWN VOLTAGE MEASUREMENT

Breakdown voltage measurements are conducted using oil tester BAUR DTA 100 C. The method of applying and measuring voltage is the same for all tests. After the sample positioning and distance setting, a wait time of ten minutes is respected before running the test. According to the IEC 60156 [53], the electrodes consist of two spheres of 12.5mm diameter, separated by a distance of 2.5mm. The other electrode gaps were ensured using hold plates ranging from 0.1 to 2.0mm. The voltages increment is 2kV/s until the breakdown occurs. Two minutes between each measure and the next are respected for all series; each series consists of six measurements. Three NF samples are prepared and tested for each concentration. Thus, each type of NF is subjected to three series of tests (that is a total of 18 measurements). After each series (i.e. 6 measurements), the NF sample is changed.

So, for statistical analysis, we should have sufficient data for specific electrode sets and concentrations. Hence, three series are measured for a distance of 2mm (breakdown in case of NFs do not occur with 2.5mm, AC-BDV $>$ 100kV). The AC-BDV data were then analyzed using Weibull and normal distributions. Those methods are the most used for analyzing the AC-BDV so far. Finally, the voltages corresponding to the cumulative probability of 1% and 50% are determined, and the p-value is calculated.

E. PARTIAL DISCHARGES MEASUREMENT UNDER AC 50 Hz STRESS

The partial discharges (PDs) activity in both SE and SE-based C_{60} and Gr NFs at optimal concentration is conducted in compliance with IEC 60270 standard method using an industrial Omicron PDs system detection. The PDs test is performed in a needle-plane electrodes configuration with a gap spacing of 5mm. The tip radius of curvature is 10μm, while the plane electrode has a 30mm diameter. Figure 7 shows the profile of the voltage RMS value applied to all samples; the voltage

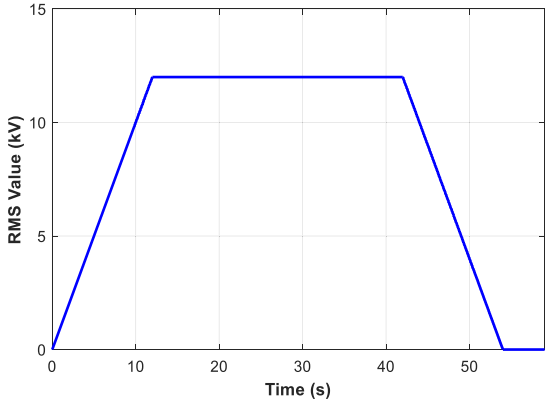

FIGURE 7. Voltage profile (RMS value) applied to samples.

rises and falls with 1kV/s speed, 12kV as the maximum value, kept for 30s, and 5s of rest is respected between two successive tests. This voltage profile is applied five times for each sample, which that underwent five PDs tests for each liquid. A microscope monitoring of the needle tip before and after demonstrates that those series of PDs tests does not affect the condition of the needle.

During the tests, the PDs inception voltages (PDIVs), extinction voltages (PDEVs), average charge (Qavg), peak charge (Qpeak), and number of PDs (NPDs/s) are measured. Note that Qavg represents the average of the PDs charge magnitude and NPD/s the number of PDs per second during the 30s of the maximum applied voltage. In addition, the phase-resolved PDs pattern is also compared for the three liquids.

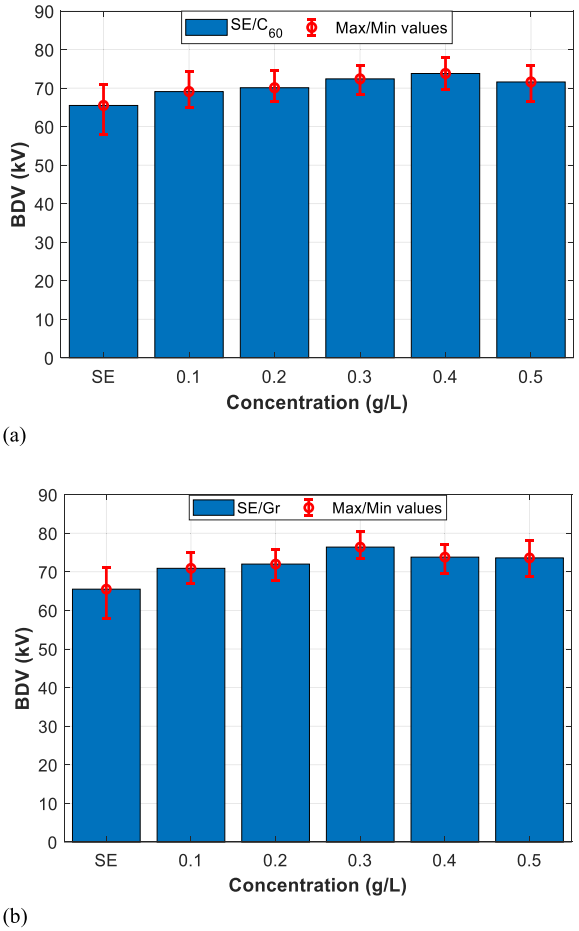

FIGURE 8. Mean breakdown voltages of different nanofluids for a given distance (d = 2mm); (a) with C_{60} and (b) with Gr.

III. RESULTS

A. MEAN VALUE OF BREAKDOWN VOLTAGE

The mean value of the voltage and standard deviation of each series are calculated according to equations (1) and (2).

$$U_{mean} = \frac{1}{n}\sum_{i=1}^{n}(U)_i \tag{1}$$

$$St.Dev(kV) = \sqrt{\frac{1}{n}\sum_{i=1}^{n}\left[(U)_i - U_{mean}\right]^2} \tag{2}$$

U_i is the measured voltage, and "n" is the number of tests per series. According to the IEC 60156, "n" refers to number of tests per series.

Figures 8. (a) and 8. (b) give the mean values of BDV for different SE-based NFs with fullerene (C_{60}) and graphene (Gr), respectively, for a specific distance equal to 2mm. We have mentioned before that the BDs does not occur for a 2.5mm gap distance because of the 100kV limitation of oil tester.

It is noticed that SE-based NFs with C_{60} reach the highest BDV value for a concentration of 0.4 g/L (Figure 8. (a)), which presents a 12.67% of improvement against pure SE. While with graphene, the best enhancement is about 16.64% for 0.3 g/L, as shown in figure 8. (b). Moreover, for d = 2mm, the BDV is enhanced whatever the concentration of NFs, the nature of NPs with respect to SE. Furthermore, this improvement depends on the type and concentration of nanoparticles. Hence, figure 8 highlights the optimal concentration concept as reported in [5], [13], [54]. Note that with SE-based C_{60} NFs, beyond the optimal concentration (0.4 g/L), BDV seems to tend to decrease, while with graphene, this is observed beyond 0.3 g/L.

The results presented previously in figure 8 were now presented numerically in Table 4 with standard deviation (Std.) values of NFs for different concentrations of NPs. Besides improving the breakdown voltage mean value, the addition of nanoparticles provides a decreased standard deviation, mainly providing a high peak on the normal distribution histogram plot. A detailed explanation will be considered in the coming paragraphs. Thus, the slightest standard deviation was the highest peak will. In addition, the slight standard deviation provides better transformer reliability, in which the breakdown voltage at very weak cumulative probability will be enhanced.

TABLE 4. Mean breakdown voltages and standard deviation values of different nanofluids for a given distance (d = 2mm).

Concentration		SE	Fullerene (C_{60})	Graphene (Gr)
0.1 (g/L)	BDV (kV)	65.5	69.1	70.9
	St. Dev (kV)	7.5	4.2	5.0
	Increment %	–	5.49	8.24
0.2 (g/L)	BDV (kV)	65.5	70.1	72.0
	St. Dev (kV)	7.5	3.5	4.5
	Increment %	–	7.02	9.92
0.3 (g/L)	BDV (kV)	65.5	72.4	76.4
	St. Dev (kV)	7.5	4.0	4.7
	Increment %	–	10.53	16.64
0.4 (g/L)	BDV (kV)	65.5	73.8	73.8
	St. Dev (kV)	7.5	4.2	4.0
	Increment %	–	12.67	12.67
0.5 (g/L)	BDV (kV)	65.5	71.6	73.6
	St. Dev (kV)	7.5	4.7	5.6
	Increment %	–	9.31	12.36

Figure 9 depicts the percentage improvement of the AC BDV of NFs as a function of the gap distance for different concentrations. It was observed that with SE-based NFs with C_{60} (Figure 9. (a)) and Gr (Figure 9. (b)), the BDV values are increased, whatever the electrode gap and the NPs concentrations. However, the improvement is more important for SE-based NFs with C_{60} than with Gr for distances up to 0.5mm. Beyond this distance, the enhancement is more important with SE-based NFs with Gr than that with C_{60}. Such a difference may be due to the difference in the geometrical patterns of the two nanomaterials. The geometric structure of fullerene nanoparticles is a truncated icosahedron (dot, 0D), which looks like a soccer ball, while graphene is a crystalline two-dimensional (2D) material.

The fact that the improvement of BDV increases with the electrodes gap and passes by a maximum for a given gap (0.5mm with fullerene and 0.7mm for graphene) before decreasing could be due to the involved physicochemical processes which could be different for smaller electrode gaps than for the larger ones. Also, it is well known that the dielectric strength is higher for small gaps than for the long ones. The electric field can also explain these differences since beyond a certain electrodes gap distance, the electric field loses some of its uniformity in the sphere-to-sphere electrodes set. Note that the improvement in BDV with fullerene at 0.7mm is less than for other electrode gaps.

B. STATISTICAL ANALYSIS OF AC BREAKDOWN VOLTAGE

The most-reported statistical laws for analyzing the breakdown voltage data are Weibull and normal distributions. Anderson - Darling and Shapiro – Wilk conformity tests are conducted on experimental data to check their conformity with those distributions. The Anderson-Darling statistic measures how well the data follow a particular distribution. The better the distribution fits the introduced data, the smaller this statistic will be, while the Shapiro – Wilk statistic measures how well the data follow the normal distribution. The p-value computation allows checking if the data come from

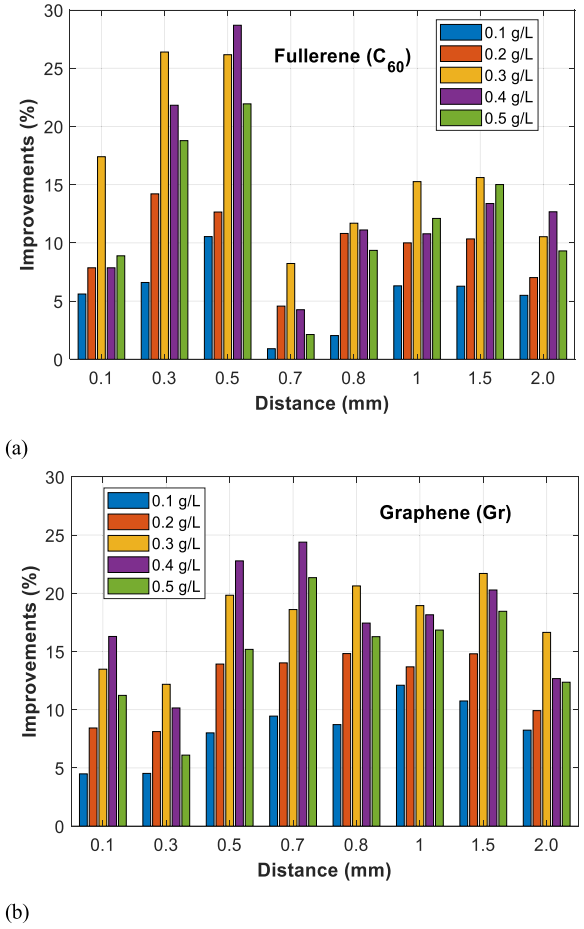

FIGURE 9. Improvements of breakdown voltages versus gap distance of different SE-based NFs with (a) C_{60} and (b) Gr.

a particular distribution. If the p-value is less than a chosen alpha (0.05), reject the null hypothesis that the data come from those distributions.

1) WEIBULL PROBABILITY ANALYSIS

Figures 10. (a) and 10. (b) show the Weibull probabilities plots of the AC BDV of SE and SE-based nanofluids with fullerene and graphene, respectively, for different concentrations of NPs, for d = 2mm. The shape, scale, number of samples (N), Anderson–Darling (AD), and p-values are shown in the supplements of these figures. The shape value, also known as the Weibull slope, indicates the slope of the linear fit characteristic, while the scale value indicates failure degree. Note that, beyond the concentration of 0.3 g/L, the slope is around ten to eleven. Thus, except at a concentration of 0.1 and 0.2 g/L with significant cumulative probability (more than 0.95), the AC BDV of NFs are higher than that of synthetic ester, whatever the nature and size of nanoparticles.

Table 5 summarizes the computed p-values for the investigated nanofluids samples and the decision about conformity to Weibull distribution. We noticed that all NFs samples obey Weibull distribution according to p-value computation.

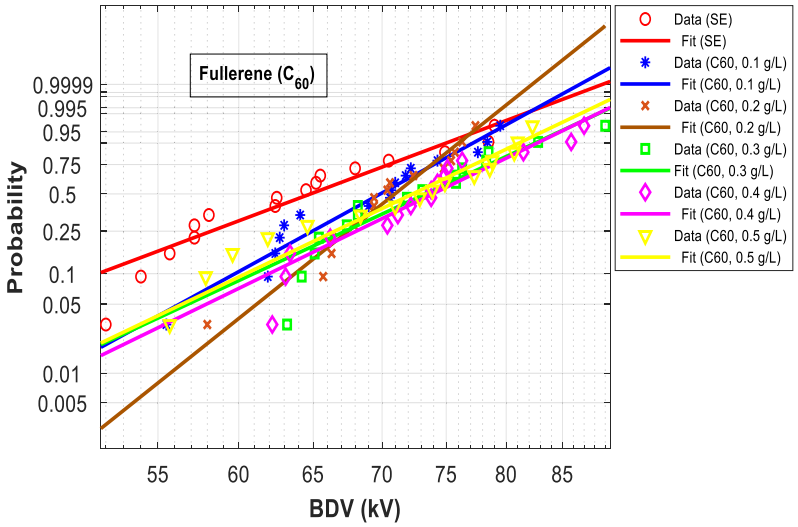

(a)

SE-based NFs with C_{60}

g/L	Shape	Scale	N	AD	p
0.1	12.66	71.94		0.38	0.39
0.2	18.77	72.54		0.31	0.54
0.3	10.53	75.84	18	0.30	0.56
0.4	11.19	76.41		0.57	0.13
0.5	11.20	74.89		0.50	0.20

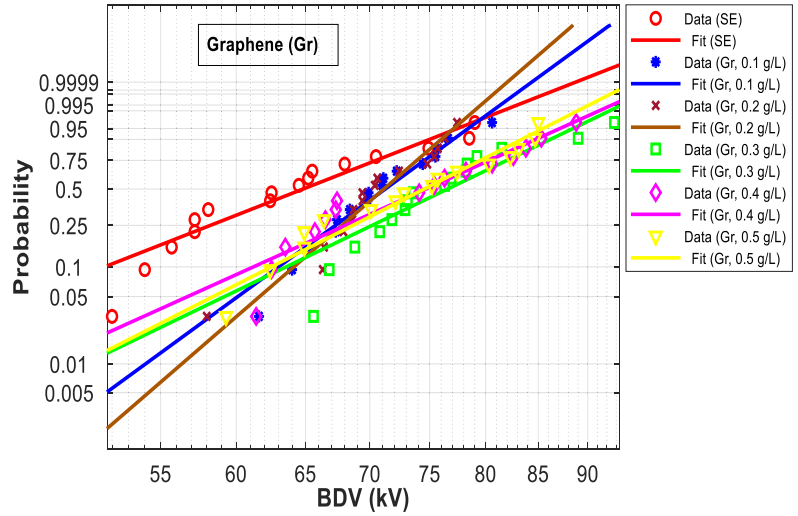

(b)

SE-based NFs with Gr

g/L	Shape	Scale	N	AD	*p*
0.1	16.20	73.09		0.14	0.97
0.2	18.61	72.37		0.57	0.14
0.3	10.53	79.24	18	0.46	0.25
0.4	9.80	77.30		0.29	0.61
0.5	11.27	77.05		0.25	0.72

FIGURE 10. Weibull probability plot of breakdown voltage data of SE-based nanofluids for an electrode gap of 2 mm, with (a) C_{60} and (b) Gr.

TABLE 5. Hypothesis test of conformity to weibull distribution considering p-value calculation of breakdown voltage outcomes of various nanofluids.

		p-value	Decision
	SE	0.51	Accepted
SE-based C_{60}	**(0.1 g/L)**	0.38	Accepted
	(0.2 g/L)	0.31	Accepted
	(0.3 g/L)	0.30	Accepted
	(0.4 g/L)	0.57	Accepted
	(0.5 g/L)	0.50	Accepted
SE-based Gr	**(0.1 g/L)**	0.97	Accepted
	(0.2 g/L)	0.14	Accepted
	(0.3 g/L)	0.25	Accepted
	(0.4 g/L)	0.61	Accepted
	(0.5 g/L)	0.72	Accepted

Table 6 gives the AC breakdown voltages at 1% and 50% cumulative probability for the two studied NFs, deduced from Weibull distribution plots. This table shows the voltage for each probability and the enhancement of NFs concerning SE. In most cases, nanofluids BDV was higher than that of SE, regardless of the type and concentrations of NPs; Khaled et Beroual [4] reported such results in the case of SE-based NFs with metals oxides NPs. The addition of nanoparticles significantly improves the 1% probability BDV, and this improvement can reach 50% in the case of SE-based NFs with graphene at a concentration of 0.3g/L. However, the same type and concentration of NPs allow having the best improvement in the mean value.

2) SHAPIRO-WILK NORMALITY TEST

Figures 11 and 12 give the histograms of the breakdown voltage distribution of the tested samples for an electrode gap of d = 2mm. Those histograms can give a general idea of the shape. It is observed at first glance that the experimental data also obey the normal distribution. To confirm this

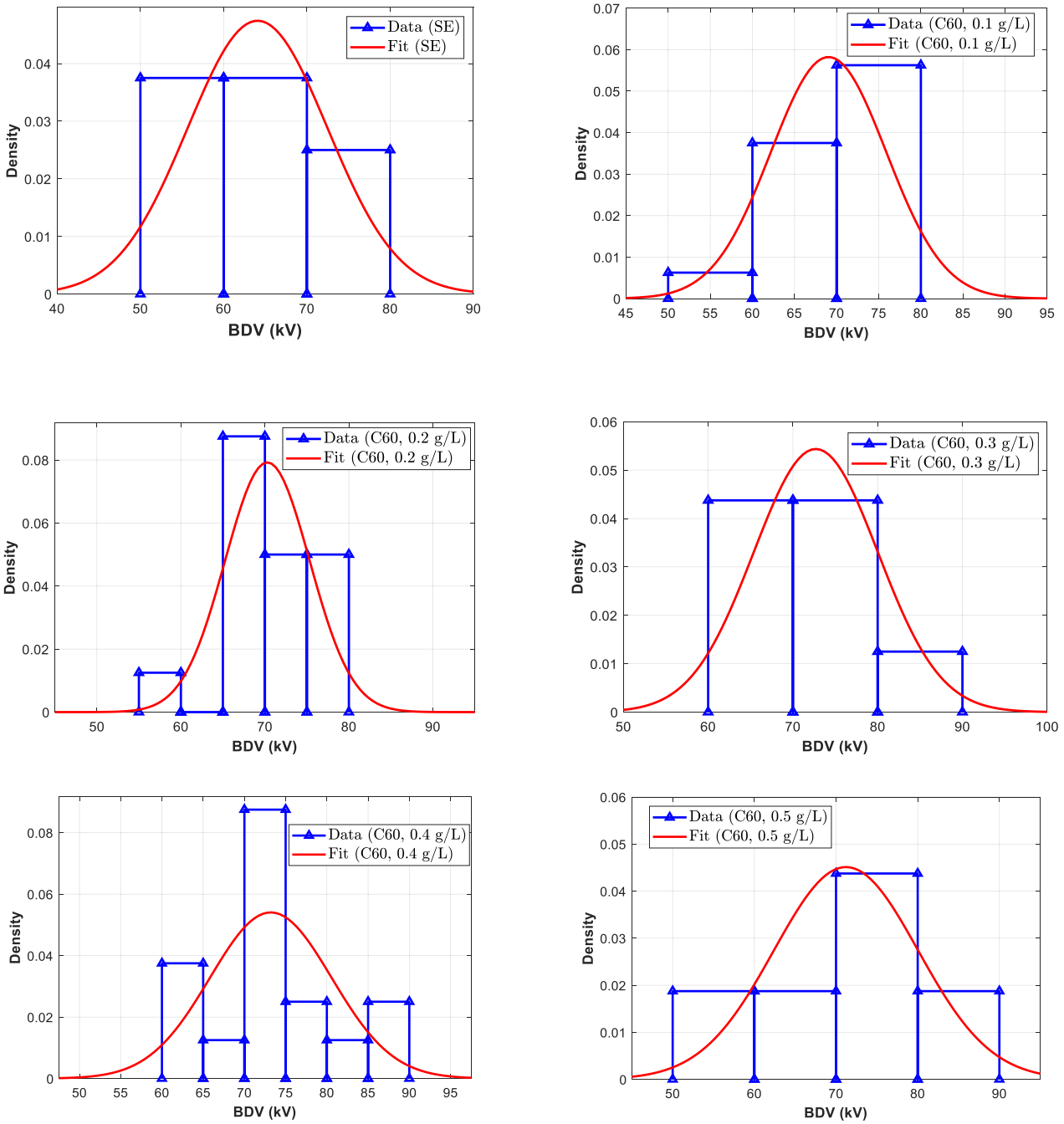

FIGURE 11. Histograms of synthetic ester and synthetic ester-based nanofluids with fullerene for different concentrations for d = 2mm.

conformity, two numerical measures of shape provide a more precise evaluation which is called 'measures of shape,' and more precisely, 'Skewness and Kurtosis': Skewness indicates the amount and direction of skew (deviation from horizontal symmetry), and Kurtosis indicates how tall, and sharp the central peak is relative to a standard bell curve. Hence, to prove normal univariate distribution, skewness and Kurtosis values should be between -3 and $+3$ [4], and they are equal to zero in the case of standard normal distribution. Matlab software was used to compute these two parameters, and the results are depicted in Table 7. It appears that except SE/C_{60} (0.2$_g$/L) and SE/Gr (0.2 and 0.3$_g$/L) nanofluids cases, for which their Kurtosis is higher than three, all other samples provide satisfactory Kurtosis values. However, according to Khaled et Beroual [4], Kurtosis values higher than three do not exclude the data from normality. Furthermore, all Kurtosis values are positive. These distributions with positive Kurtosis values are called leptokurtic distribution,

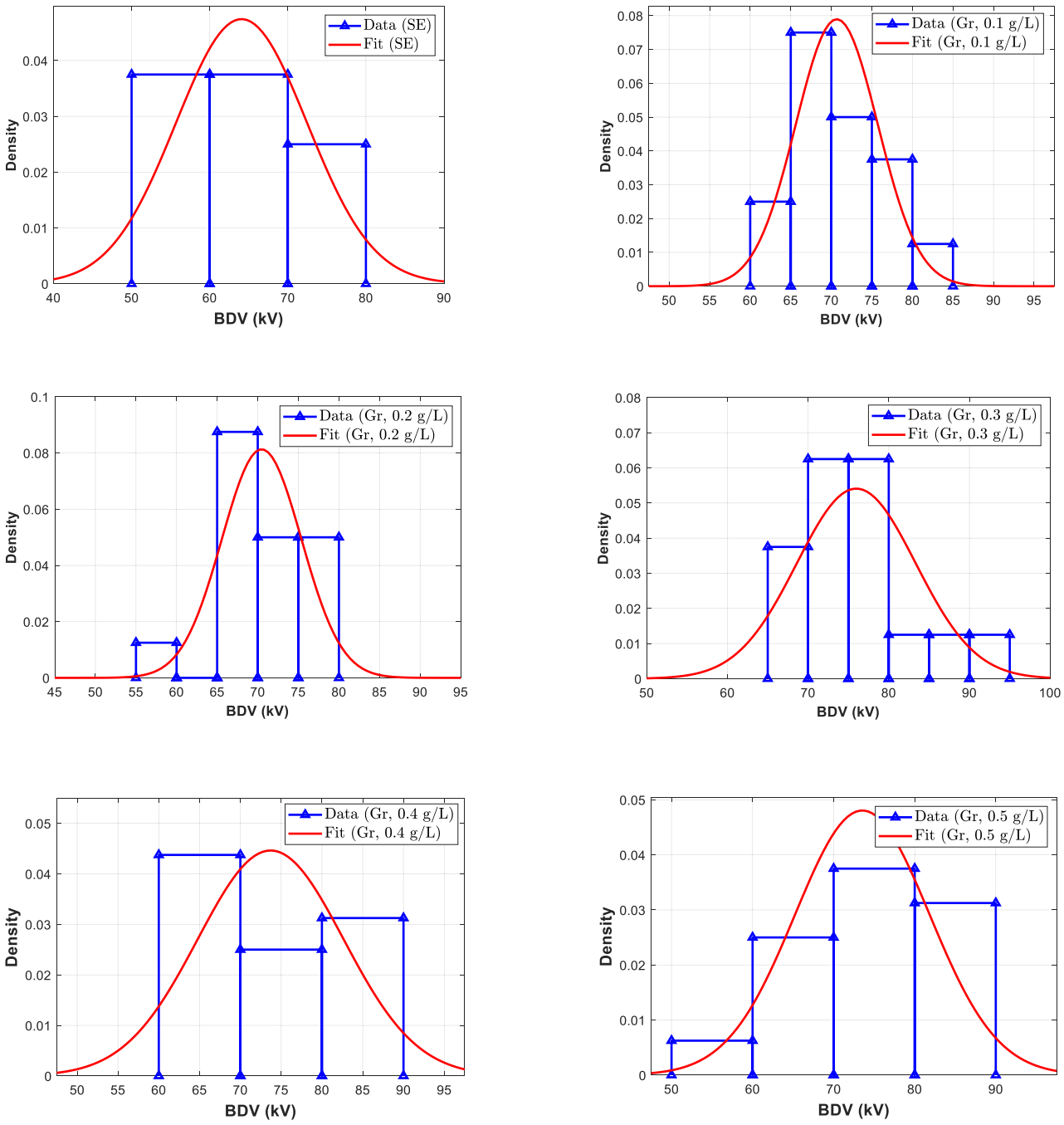

FIGURE 12. Histograms of synthetic ester and synthetic ester-based nanofluids with graphene for different concentrations for d = 2mm.

with a high peak, resulting in a small standard deviation value.

Nevertheless, the Shapiro-Wilk normality test on the experimental data should be conducted via p-value to verify the conformity with normal distribution. Therefore, the Matlab program was extended to compute those values and compare them with the alpha value.

Table 8 summarizes the p-values for investigated NFs samples and the conformity to normal distribution. We observe that the p-value calculated for the experimental data for SE and SE-based NFs with fullerene and graphene are higher than the significance value ($\alpha = 0.05$). Thus, they do all obey normal distribution. Furthermore, we observe that with all SE-based NFs with Gr (0.1 g/L) whose p-value is close to

TABLE 6. AC breakdown voltages at 1% and 50% cumulative probability for various nanofluids.

		1%		50%	
		BDV (kV)	Increment (%)	BDV (kV)	Increment (%)
	SE	43.99	–	64.10	–
SE-based C_{60}	**(0.1 g/L)**	53.10	20.70	69.05	7.72
	(0.2 g/L)	58.58	33.16	70.31	9.68
	(0.3 g/L)	55.64	26.48	72.70	13.41
	(0.4 g/L)	56.02	27.34	73.20	14.19
	(0.5 g/L)	59.89	36.14	71.22	11.10
SE-based Gr	**(0.1 g/L)**	64.20	45.94	70.70	10.29
	(0.2 g/L)	64.22	45.98	70.50	9.98
	(0.3 g/L)	66.53	51.23	75.98	18.53
	(0.4 g/L)	62.28	41.57	73.72	15.00
	(0.5 g/L)	62.9	42.98	73.54	14.72

TABLE 7. Skewness and kurtosis of the breakdown voltage of SE and SE-based nanofluids.

Concentration	Skewness	Kurtosis
SE	+0.42	2.14
SE-based NFs with fullerene		
0.1 g/L	–0.20	2.18
0.2 g/L	–0.60	3.27
0.3 g/L	+0.55	2.56
0.4 g/L	+0.26	2.47
0.5 g/L	–0.44	1.83
SE-based NFs with graphene		
0.1 g/L	+0.10	2.41
0.2 g/L	–0.72	3.68
0.3 g/L	+0.80	3.18
0.4 g/L	+0.13	1.65
0.5 g/L	–0.13	1.79

TABLE 8. Hypothesis test of conformity to normal distribution considering p-value calculation of breakdown voltage outcomes of various nanofluids.

	p-value	Decision
SE	0.50	Accepted
SE-based NFs with fullerene		
(0.1 g/L)	0.49	Accepted
(0.2 g/L)	0.32	Accepted
(0.3 g/L)	0.36	Accepted
(0.4 g/L)	0.34	Accepted
(0.5 g/L)	0.15	Accepted
SE-based NFs with graphene		
(0.1 g/L)	0.99	Accepted
(0.2 g/L)	0.18	Accepted
(0.3 g/L)	0.30	Accepted
(0.4 g/L)	0.27	Accepted
(0.5 g/L)	0.45	Accepted

unity, the normal distribution fits perfectly the experimental data.

C. AC (50Hz) PARTIAL DISCHARGES ACTIVITY OF SE-BASED FULLERENE (C_{60}) AND GRAPHENE (Gr)

Table 9 presents the average and standard deviation of PDIVs, PDEVs, Qavg, Qpeak, and NPDs/s values obtained from electrical measurement for different liquids tested with a threshold level of 2pC. The depicted values are the average of five underwent tests on each liquid. The PDIVs values of

TABLE 9. PD activity of synthetic ester and synthetic ester -based nanofluids with fullerene and graphene.

	SE	SE/Fullerene	SE/Graphene
PDIVs (kV)	10.476	11.015	6.983
Std. (kV)	0.58	0.362	0.582
Enhancement (%)	–	+5.1	-33.34
PDEVs (kV)	8.070	6.861	4.890
Std. (kV)	0.732	1.481	0.387
Enhancement (%)	–	-14.98	-39.40
Qavg (pC)	14.3	11.7	124.4
Std. (pC)	1	1	5
Enhancement (%)	–	+18.18	-770
Qpeak (pC)	205	134	573
Std. (pC)	68	9	67
Enhancement (%)	–	+34.63	-180
NPDs (PDs/s)	42	24	250
Std. (PDs/s)	2	1	3
Enhancement (%)	–	+42	-495

SE-based NF with C_{60} at 0.4 g/L are higher than that in pure SE. The opposite is observed with SE-based Gr NF at 0.3 g/L, which presents a poor PDIVs value. In the case of fullerene, this was enhanced by about 5.1% and was worsened by about 33.33% with graphene. Furthermore, the lower Qavg, Qpeak, and NPDs/s for SE-based C_{60} NF demonstrates that fullerene NPs enhanced the performance of the SE liquid with a lower PDs activity. On the other hand, graphene NPs deteriorates the fluid behavior increasing the PDs activity at the same voltage level. The PDEVs results show that the pure SE gives the best extinction voltage compared to the two NFs. It was decreased by about 14.98% with C_{60} and by about 39.4% with Gr.

Figures 13 – 15 show the PDs patterns of SE, SE-based NF with C_{60} at 0.4 g/L, and SE-based NF with Gr at 0.3 g/L, respectively, at 12kV (RMS) voltage level after 30s. For all three cases, it was observed that the PDs activity began with the appearance of PDs at the peak of negative polarity (270° electrical degrees), and just after at the peak of positive polarity (90° electrical degrees) with less number of PDs but a higher charge level. Furthermore, it was noticed that C_{60} NF (Figure 14) shows the lowest activity in terms of PDs activity compared to pure SE. However, unlike C_{60}, Gr NF exhibits the more important PDs activity, both at the positive and negative polarities. Based on partial discharge measurements, with a higher PDIV and a lower PDs activity, it can be said that the addition of fullerene NPs enhances the performance of the pure liquid against PDs activity.

IV. DISCUSSION

A. AC BRE AKDOWN VOLTAGE OF FULLERENE AND GRAPHENE NANOFLUIDS

Conformity check-in of two statistical laws was conducted on our samples using the p-value calculation for one specific

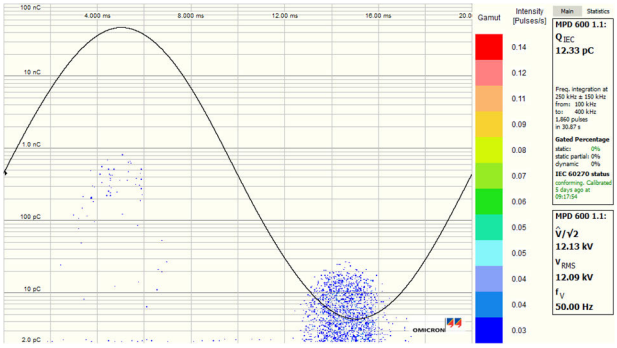

FIGURE 13. PD pattern pure synthetic ester (MIDEL 7131) at 12kV voltage level.

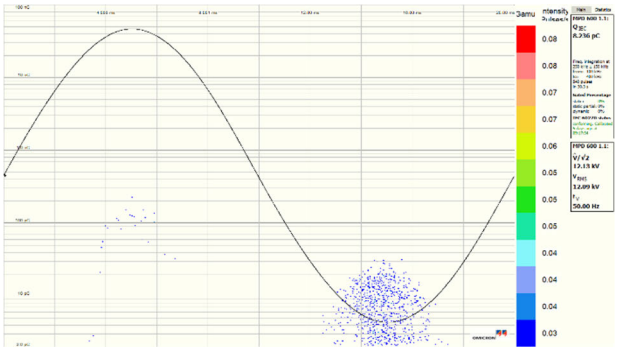

FIGURE 14. PD pattern synthetic ester-based NF with fullerene at 12kV voltage level.

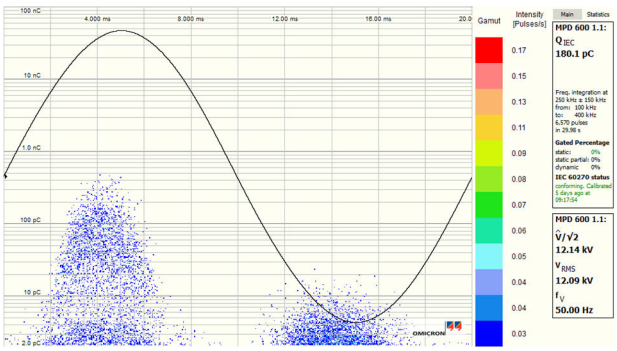

FIGURE 15. PD pattern synthetic ester-based NF with graphene at 12kV voltage level.

gap distance. Then, these values were compared to the significance value ($\alpha = 5\%$) to validate the conformity. It appears from those results that the experimental data of breakdown voltages for all investigated nanofluids samples obey both Weibull and normal distributions. Thus, these results confirm those reported by elsewhere in which breakdown voltages data of nanofluids and their host liquids usually obey normal and Weibull distributions [5], [13], [20].

It was noticed from experimental results that SE-based nanofluids with fullerene (C_{60}) and graphene (Gr) show an increased breakdown voltage compared to pure host synthetic ester (SE) under AC stress. For a given distance equal to 2mm, regardless of the concentration, SE-based NFs with Gr show a noteworthy improvement than SE-based NFs with C_{60}. These improvements are between 5.5 and 12.67% with C_{60} and 8.25 and 16.64% with Gr. The improvement depends not only on the nature and the concentration of nanoparticles but also on the gap distance. For most cases, from 0.1 to 0.5mm, the improvement is more important with SE-based NFs with C_{60} than that with Gr, and the optimal improvement is about 28.7% at 0.5mm; beyond 0.5mm, the SE-based NFs with Gr becomes more important and op^{2}timal enhancement reach 24.39% at 0.7mm. The existence of an optimal concentration for each kind of NPs could be due to the saturation of interfaces between NPs and hosting liquid by electrons. The trapping and accumulation of moving electrons would have reached a limit that the NPs interfaces cannot exceed.

In addition, the presence of NPs improves the AC breakdown voltages at 1% and 50% cumulative probability. Since unexpected collapse at a low voltage value must be considered, each sample breakdown voltage at the lowest probability (1%) is crucial for transformer safety. Therefore, it was observed that NFs with C_{60} and Gr have shown an enhanced breakdown strength against pure SE at the lowest probability, especially with Gr. At 0.3 g/L of Gr NF, the best enhancement reaches 51.23%. While, with 0.5 g/L of C_{60} NF, the best improvement of breakdown voltage was about 36.14%. Those results confirm the high safety of the nanofluid with Gr and C_{60}.

Many research works are engaged to understand better the mechanisms/reasons responsible for improving breakdown voltage in the presence of nanoparticles, and there is almost total unanimity that the nanostructures affect the streamers development. Thus, Peppas *et al.* [20] tend to explain the improvement in the dielectric strength with the presence of NPs by the efficient electrons trapping resulting by nanostructures, which frustrates the development of streamers and reduces their propagation speed. On the other hand, Ibrahim *et al.* [5] studied the effect of particles charge on the breakdown phenomena in AC and DC stress for the first time. They conduce that the positively charged nanoparticle holds positive charges that can trap the streamer electrons. Therefore, it increases the breakdown strength of the NF. Conversely, negatively charged particles catch the electrons from the ionized oil molecules to the positive charges formed due to polarization.

A multi-core model was proposed by Tanaka *et al.* [55] in solid dielectrics and, more particularly, to analyze different phenomena that polymer nanocomposite dielectrics exhibit, which provides a fine structure to ‘‘interaction zones.’’. This model was served by Atiya *et al.* [50]. They suggest that the breakdown voltage improvement was due to the interfacial region formed around the nanoparticle. Based on the electronegativity of nanoparticles, the breakdown mechanism was proposed by preventing streamer propagation into the first and second modes, and fast-moving electrons are trapped. Hence the breakdown process is delayed.

Most authors have proposed those mechanisms/reasons, and others suggest that the conductivity of nanoparticles could be one of the reasons for delaying streamer development. Through an experimental study on insulation performances of transformer oil-based NFs with conductive Fe_3O_4, semi-conductive TiO_2, and insulating Al_2O_3 nanoparticles, Sima *et al.* [14] proposed an ionization model of NFs. According to this model, the conductive NPs reduce the mobility of fast-moving electrons and turn them into sluggish negative charged NPs, resulting in slowing streamer propagation. Khaled and Beroual [4] tested SE-based NFs with two types of NPs, conductive (Fe_3O_4) and insulating (Al_2O_3 and SiO_2). They observed that conductive nanoparticles (Fe_3O_4) give better enhancement than insulating nanoparticles (SiO_2 and Al_2O_3). While insulating particles give fairly the same improvements of breakdown voltage. The same authors studied AC BDV of Mineral oil-based and synthetic and natural esters NFs with Fe_3O_4 [13]. The presence of Fe_3O_4 has doubled the BDV with mineral oil and improved it by about 48 and 7% with SE and NE, respectively. This work showed that the nature of liquid is a fundamental factor in the improvements of BDV. In addition to the conductivity of NPs, according to Hwang *et al.* [22], the dielectric constants of base liquid and nanoparticles explained the breakdown voltage enhancement. NPs and base liquids having close conductivities and dielectric constants cause the breakdown voltage to deteriorate; the further apart these two parameters are, the higher the breakdown voltage of NF will be.

The enhancement of breakdown voltage of SE when adding C_{60} and Gr we observed are likely due to their conductivities too higher than that of the base synthetic ester liquid confirming thence the results reported elsewhere [4], [14] and to the difference in dielectric permittivities of graphene (about 6.9) and fullerene (2.2) regarding that of SE (3.2) as suggested by Hwang *et al.* [22]. The fact that graphene gives slightly better improvement of BDV than fullerene can be due to its higher dielectric permittivity. Also, the geometry of fullerene and graphene molecules make those molecules can act at two levels (1) as barriers in the vicinity of electrodes by reducing the injected charges into the fluid, increasing thence the initiation threshold voltage of streamers/discharges and therefore the breakdown voltage; and (2) by capturing the moving streamer electrons thence delaying the breakdown.

B. PDs ACTIVITY OF FULLERENE AND GRAPHENE NANOFLUIDS

It emerges from the above results that the addition of Fullerene NPs to SE significantly reduces the activity of PDs, unlike graphene, which tremendously destroys the PDs resistance of pure SE. The addition of C_{60} increases the PDIV and reduces Qavg, Qpeak, and NPDs/s compared to the reference SE under AC stress, while Gr NF shows poor performances regarding to PDs activity. It was mentioned previously that the conductive NPs reduce the mobility of fast-moving electrons and turn them into sluggish negative charged NPs, resulting in slowing streamer propagation [14]. According to Atiya *et al.* [18], the electrical double layer (EDL) around the NPs captures the charge carriers, thus delaying charge accumulation via the electrode space. Therefore, since fullerene and graphene NPs are both highly conductive, it would be expected, according to this hypothesis, that both types of NPs have a favorable impact, i.e. a reduction of the activity of PDs, a slowing down the streamer development, and thence increasing the BDV. However, that is not the case: the C_{60} NPs show a very favorable effect on the activity of the PDs in SE, unlike the Gr NPs. The inception voltage of PDs with fullerene is higher than that with graphene. The other explanation for this difference could be the shape of nanoparticles. NPs of C_{60} that are spherical could capture more charge carriers than Gr NPs, which are lamellar (Gr). Jin *et al.* [16] compared the effect of hydrophilic (SiO_2) and hydrophobic (C_{60}) NPs on the PDs activity in mineral oil. They assume that the remarked difference in the inception voltage may be due to the hydrophilic behavior of silica NPs. These latter can reduce the moisture content improving hence PDs resistivity. The same authors also verified the ability to reduce moisture content when adding hydrophilic NPs (SiO_2) to mineral oil [56]. In this study, C_{60} and Gr NPs are hydrophobic, and to correctly state the effect of moisture content on the PDs activity, the water content of the three liquids (i.e. SE, SE-based C_{60} NF, and SE-based Gr NF) was measured twice using Mettler Toledo titrator. The obtained results show that the addition of C_{60} at 0.4g/L and Gr at 0.3 g/L, increases the water content of pure SE from 33.3 to 39.2 and 46.7ppm, respectively. However, these slight differences remain far from the limit value for water content, which are 200ppm for new Midel 7131 and 400ppm for Midel 7131 in service, according to standard IEC 61099 and IEC 61203, respectively. Hence, those results do not allow such a conclusion to be drawn on the effect of the water content on the PDs activity of SE-based NF.

V. CONCLUSION

To infer, an experimental study on the effect of two carbonic nanomaterials (namely, fullerene and graphene) on the AC breakdown voltages and partial discharges activity of synthetic ester (Midel 7131)-based nanofluids has been presented. It showed that adding Gr and C_{60} NPs at different concentrations improves the AC breakdown voltages. However, the improvement depends not only on the concentration but also on the electrodes gap. Indeed, from 0.1 to 0.5mm, the enhancement is more significant with SE-based NFs with fullerene (C_{60}) than that with graphene (Gr), and the optimal improvement is about 28.7% at 0.5mm; beyond 0.5mm, the SE-based NFs with Gr becomes more interesting and optimal enhancement reach 24.39% at 0.7mm.

The statistical analysis of the experimental results performed for a gap distance of 2mm, shows that the breakdown voltage data obey the normal and Weibull probabilistic laws. Note that we considered the gap distance of 2mm, the closest to the standardized distance of 2.5 mm, because of the

limitation of the voltage supply (100 kV) and the fact that the breakdown did not occur for 2.5 mm.

It also showed that the addition of C_{60} significantly reduces the partial discharge activity in SE while the addition of Gr destroys the partial discharge resistance of pure SE.

REFERENCES

[1] S. U. Choi and J. A. Eastman, *Enhancing Thermal Conductivity of Fluids With Nanoparticles*. Lemont, IL, USA: Argonne National Lab, 1995.

[2] M. Mehrali, E. Sadeghinezhad, S. Tahan Latibari, M. Mehrali, H. Togun, M. N. M. Zubir, S. N. Kazi, and H. S. C. Metselaar, "Preparation, characterization, viscosity, and thermal conductivity of nitrogen-doped graphene aqueous nanofluids," *J. Mater. Sci.*, vol. 49, no. 20, pp. 7156–7171, Oct. 2014, doi: 10.1007/s10853-014-8424-8.

[3] P. Dhar, A. Chattopadhyay, L. S. Maganti, and A. R. Harikrishnan, "Streamer evolution arrest governed amplified AC breakdown strength of graphene and CNT colloids," *Eur. Phys. J. Appl. Phys.*, vol. 85, no. 3, p. 30402, Mar. 2019, doi: 10.1051/epjap/2019180360.

[4] U. Khaled and A. Beroual, "AC dielectric strength of synthetic ester-based Fe_3O_4, Al_2O_3 and SiO_2 nanofluids—Conformity with normal and Weibull distributions," *IEEE Trans. Dielectr. Electr. Insul.*, vol. 26, no. 2, pp. 625–633, Apr. 2019, doi: 10.1109/TDEI.2018.007759.

[5] M. E. Ibrahim, A. M. Abd-Elhady, and M. A. Izzularab, "Effect of nanoparticles on transformer oil breakdown strength: Experiment and theory," *IET Sci. Meas. Technol.*, vol. 10, no. 8, pp. 839–845, Nov. 2016, doi: 10.1049/iet-smt.2016.0104.

[6] H. Duzkaya and A. Beroual, "Statistical analysis of AC dielectric strength of natural ester-based ZnO nanofluids," *Energies*, vol. 14, no. 1, p. 99, Dec. 2020, doi: 10.3390/en14010099.

[7] W. Yu and H. Xie, "A review on nanofluids: Preparation, stability mechanisms, and applications," *J. Nanomater.*, vol. 2012, pp. 1–17, Jul. 2012.

[8] Z. Huang, J. Li, W. Yao, F. Wang, F. Wan, Y. Tan, and M. A. Mehmood, "Electrical and thermal properties of insulating oil-based nanofluids: A comprehensive overview," *IET Nanodielectr.*, vol. 2, no. 1, pp. 27–40, Mar. 2019, doi: 10.1049/iet-nde.2018.0019.

[9] N. A. Azizie and N. Hussin, "Preparation of vegetable oil-based nanofluid and studies on its insulating property: A review," *J. Phys., Conf. Ser.*, vol. 1432, no. 1, Jan. 2020, Art. no. 012025, doi: 10.1088/1742-6596/1432/1/012025.

[10] P. Thomas, N. E. Hudedmani, R. T. A. R. Prasath, N. K. Roy, and S. N. Mahato, "Synthetic ester oil based high permittivity $CaCu_3Ti_4O_{12}$ (CCTO) nanofluids an alternative insulating medium for power transformer," *IEEE Trans. Dielectr. Electr. Insul.*, vol. 26, no. 1, pp. 314–321, Feb. 2019, doi: 10.1109/TDEI.2018.007728.

[11] U. Khaled and A. Beroual, "Comparative study on the AC breakdown voltage of transformer mineral oil with transformer oil-based Al_2O_3 nanofluids," in *Proc. IEEE Int. Conf. High Voltage Eng. Appl. (ICHVE)*, Sep. 2018, pp. 1–4.

[12] M. R. Hussain, Q. Khan, A. A. Khan, S. S. Refaat, and H. Abu-Rub, "Dielectric performance of magneto-nanofluids for advancing oil-immersed power transformer," *IEEE Access*, vol. 8, pp. 163316–163328, 2020, doi: 10.1109/ACCESS.2020.3021003.

[13] U. Khaled and A. Beroual, "Influence of conductive nanoparticles on the breakdown voltage of mineral oil, synthetic and natural ester oil-based nanofluids," in *Proc. IEEE 20th Int. Conf. Dielectr. Liquids (ICDL)*, Jun. 2019, pp. 1–4.

[14] W. Sima, J. Shi, Q. Yang, S. Huang, and X. Cao, "Effects of conductivity and permittivity of nanoparticle on transformer oil insulation performance: Experiment and theory," *IEEE Trans. Dielectr. Electr. Insul.*, vol. 22, no. 1, pp. 380–390, Feb. 2015, doi: 10.1109/TDEI.2014.004277.

[15] H. Jin, P. Morshuis, A. R. Mor, J. J. Smit, and T. Andritsch, "Partial discharge behavior of mineral oil based nanofluids," *IEEE Trans. Dielectr. Electr. Insul.*, vol. 22, no. 5, pp. 2747–2753, Oct. 2015, doi: 10.1109/TDEI.2015.005145.

[16] H. Jin, P. H. F. Morshuis, A. R. Mor, and T. Andritsch, "An investigation into the dynamics of partial discharge propagation in mineral oil based nanofluids," in *Proc. IEEE 18th Int. Conf. Dielectr. Liquids (ICDL)*, Jun. 2014, pp. 1–4.

[17] E. G. Atiya, D.-E. A. Mansour, and M. A. Izzularab, "Partial discharge activity of Al_2O_3 nanofluid impregnated paper insulation system," in *Proc. Int. Symp. Electr. Insulating Mater. (ISEIM)*, Sep. 2020, pp. 379–382.

[18] E. G. Atiya, D.-E.-A. Mansour, and M. A. Izzularab, "Partial discharge development in oil-based nanofluids: Inception, propagation and time transition," *IEEE Access*, vol. 8, pp. 181028–181035, 2020, doi: 10.1109/ACCESS.2020.3027905.

[19] M. T. Imani, P. Werle, J. F. Miethe, and N. C. Bigall, "Magnetite nanofluid as alternative for conventional insulating liquids," in *Proc. IEEE 19th Int. Conf. Dielectr. Liquids (ICDL)*, Jun. 2017, pp. 1–4.

[20] G. D. Peppas, V. P. Charalampakos, E. C. Pyrgioti, M. G. Danikas, A. Bakandritsos, and I. F. Gonos, "Statistical investigation of AC breakdown voltage of nanofluids compared with mineral and natural ester oil," *IET Sci. Meas. Technol.*, vol. 10, no. 6, pp. 644–652, Sep. 2016, doi: 10.1049/iet-smt.2016.0031.

[21] Y. Lv, M. Rafiq, C. Li, and B. Shan, "Study of dielectric breakdown performance of transformer oil based magnetic nanofluids," *Energies*, vol. 10, no. 7, p. 1025, Jul. 2017, doi: 10.3390/en10071025.

[22] J. G. Hwang, M. Zahn, F. M. O'Sullivan, L. A. A. Pettersson, O. Hjortstam, and R. Liu, "Effects of nanoparticle charging on streamer development in transformer oil-based nanofluids," *J. Appl. Phys.*, vol. 107, no. 1, Jan. 2010, Art. no. 014310, doi: 10.1063/1.3267474.

[23] V. Segal, A. Hjortsberg, A. Rabinovich, D. Nattrass, and K. Raj, "AC (60 Hz) and impulse breakdown strength of a colloidal fluid based on transformer oil and magnetite nanoparticles," in *Proc. Conf. Rec. IEEE Int. Symp. Electr. Insul.*, Jun. 1998, pp. 619–622.

[24] M. Rafiq, C. Li, Y. Lv, K. Yi, and Q. Sun, "Breakdown characteristics of mineral oil based magnetic nanofluids," in *Proc. IEEE Int. Conf. High Voltage Eng. Appl. (ICHVE)*, Sep. 2016, pp. 1–4.

[25] B. Du, J. Li, B.-M. Wang, and Z.-T. Zhang, "Preparation and breakdown strength of Fe_3O_4 nanofluid based on transformer oil," in *Proc. Int. Conf. High Voltage Eng. Appl.*, Sep. 2012, pp. 311–313.

[26] P. Dhar, A. Katiyar, L. S. Maganti, A. Pattamatta, and S. K. Das, "Superior dielectric breakdown strength of graphene and carbon nanotube infused nano-oils," *IEEE Trans. Dielectr. Electr. Insul.*, vol. 23, no. 2, pp. 943–956, Apr. 2016, doi: 10.1109/TDEI.2015.005477.

[27] P. Aksamit, D. Zmarzly, T. Boczar, and M. Szmechta, "Aging properties of fullerene doped transformer oils," in *Proc. IEEE Int. Symp. Electr. Insul.*, Jun. 2010, pp. 1–4.

[28] J. Chen, P. Sun, W. Sima, Q. Shao, L. Ye, and C. Li, "A promising nano-insulating-oil for industrial application: Electrical properties and modification mechanism," *Nanomaterials*, vol. 9, no. 5, p. 788, May 2019, doi: 10.3390/nano9050788.

[29] A. Krueger, *Carbon Materials and Nanotechnology*, 1st ed. Hoboken, NJ, USA: Wiley, 2010, doi: 10.1002/9783527629602.

[30] Y. Y. Hui, H.-C. Chang, H. Dong, and X. Zhang, *Carbon Nanomaterials for Bioimaging, Bioanalysis, and Therapy*. Chichester, U.K.: Wiley, 2019, doi: 10.1002/9781119373476.

[31] V. Campisciano, M. Gruttadauria, and F. Giacalone, "Modified nanocarbons for catalysis," *ChemCatChem*, vol. 11, no. 1, pp. 90–133, Jan. 2019, doi: 10.1002/cctc.201801414.

[32] D. Eder and R. Schlögl, *Nanocarbon-Inorganic Hybrids: Next Generation Composites for Sustainable Energy Applications*. Berlin, Germany: Walter de Gruyter, 2014.

[33] L. Dai, *Carbon Nanotechnology: Recent Developments in Chemistry, Physics, Materials Science and Device Applications*. Amsterdam, The Netherlands: Elsevier, 2006.

[34] A. Hirsch, "The era of carbon allotropes," *Nature Mater.*, vol. 9, pp. 868–871, Oct. 2010, doi: 10.1038/nmat2885.

[35] N. Yang, G. Zhao, and J. Foord, *Nanocarbon Electrochemistry*. Hoboken, NJ, USA: Wiley, 2019, p. 384.

[36] A. Khan, M. Jawaid, and A. M. Asiri, Eds., *Nanocarbon and its Composites: Preparation, Properties and Applications*. Duxford, U.K.: Woodhead Publishing, 2019.

[37] E. P. Samorì and V. Palermo, *Flexible Carbon-based Electronics*, vol. 3. Hoboken, NJ, USA: Wiley, 2018, p. 325.

[38] M. Zhou, Y.-H. Lu, Y.-Q. Cai, C. Zhang, and Y.-P. Feng, "Adsorption of gas molecules on transition metal embedded graphene: A search for high-performance graphene-based catalysts and gas sensors," *Nanotechnology*, vol. 22, no. 38, 2011, Art. no. 385502, doi: 10.1088/0957-4484/22/38/385502.

[39] A. Ghanam, A. A. Lahcen, T. Beduk, H. N. Alshareef, A. Amine, and K. N. Salama, "Laser scribed graphene: A novel platform for highly sensitive detection of electroactive biomolecules," *Biosensors Bioelectron.*, vol. 168, Nov. 2020, Art. no. 112509, doi: 10.1016/j.bios.2020.112509.

[40] Q. Xiang and J. Yu, "Graphene-based photocatalysts for hydrogen generation," *J. Phys. Chem. Lett.*, vol. 4, no. 5, pp. 753–759, Mar. 2013, doi: 10.1021/jz302048d.
[41] G. Xie, K. Zhang, B. Guo, Q. Liu, L. Fang, and J. R. Gong, "Graphene-based materials for hydrogen generation from light-driven water splitting," *Adv. Mater.*, vol. 25, no. 28, pp. 3820–3839, Jul. 2013, doi: 10.1002/adma.201301207.
[42] H. Fei, J. Dong, M. J. Arellano-Jiménez, G. Ye, N. D. Kim, E. L. G. Samuel, Z. Peng, Z. Zhu, F. Qin, J. Bao, M. J. Yacaman, P. M. Ajayan, D. Chen, and J. M. Tour, "Atomic cobalt on nitrogen-doped graphene for hydrogen generation," *Nature Commun.*, vol. 6, no. 1, p. 8668, Dec. 2015, doi: 10.1038/ncomms9668.
[43] T. Gatti, E. Menna, M. Meneghetti, M. Maggini, A. Petrozza, and F. Lamberti, "The renaissance of fullerenes with perovskite solar cells," *Nano Energy*, vol. 41, pp. 84–100, Nov. 2017, doi: 10.1016/j.nanoen.2017.09.016.
[44] C. Cui, Y. Li, and Y. Li, "Fullerene derivatives for the applications as acceptor and cathode buffer layer materials for organic and perovskite solar cells," *Adv. Energy Mater.*, vol. 7, no. 10, May 2017, Art. no. 1601251, doi: 10.1002/aenm.201601251.
[45] W. Yu and H. Xie, "A review on nanofluids: Preparation, stability mechanisms, and applications," *J. Nanomater.*, vol. 2012, pp. 1–17, Jul. 2012, doi: 10.1155/2012/435873.
[46] *User Manual ZetaSizer ZS, Nano Series*, Malvern, Almelo, The Netherlands, 2013.
[47] Y. Nakama, "Surfactants," in *Cosmetic Science and Technology*. Amsterdam, The Netherlands: Elsevier, 2017, pp. 231–244, doi: 10.1016/B978-0-12-802005-0.00015-X.
[48] R. A. Farade, N. I. A. Wahab, D.-E. A. Mansour, and N. B. Azis, "Investigation of the effect of sonication time on dispersion stability, dielectric properties, and heat transfer of graphene based green nanofluids," *IEEE Access*, vol. 9, pp. 50607–50623, 2017.
[49] D. Zhu, X. Li, N. Wang, X. Wang, J. Gao, and H. Li, "Dispersion behavior and thermal conductivity characteristics of Al_2O_3–H_2O nanofluids," *Current Appl. Phys.*, vol. 9, no. 1, pp. 131–139, Jan. 2009, doi: 10.1016/j.cap.2007.12.008.
[50] E. G. Atiya, D.-E.-A. Mansour, R. M. Khattab, and A. M. Azmy, "Dispersion behavior and breakdown strength of transformer oil filled with TiO_2 nanoparticles," *IEEE Trans. Dielectrics Electr. Insul.*, vol. 22, no. 5, pp. 2463–2472, Oct. 2015, doi: 10.1109/TDEI.2015.004742.
[51] K. N. Koutras, I. A. Naxakis, A. E. Antonelou, V. P. Charalampakos, E. C. Pyrgioti, and S. N. Yannopoulos, "Dielectric strength and stability of natural ester oil based TiO2 nanofluids," *J. Mol. Liquids*, vol. 316, Oct. 2020, Art. no. 113901.
[52] A. S. Dukhin and P. J. Goetz, *Ultrasound for Characterizing Colloids: Particle Sizing, Zeta Potential, Rheology*, 1st ed. Boston, MA, USA: Elsevier, 2002.
[53] *Insulating Liquids—Determination of the Breakdown Voltage at Power Frequency—Test Method*, document IEC 60156, Edition 3.0, International Electrotechnical Commission, 2018.
[54] M. Rafiq, C. Li, Y. Ge, Y. Lv, and K. Yi, "Effect of Fe_3O_4 nanoparticle concentrations on dielectric property of transformer oil," in *Proc. IEEE Int. Conf. High Voltage Eng. Appl. (ICHVE)*, Sep. 2016, pp. 1–4.
[55] T. Tanaka, M. Kozako, N. Fuse, and Y. Ohki, "Proposal of a multi-core model for polymer nanocomposite dielectrics," *IEEE Trans. Dielectr. Electr. Insul.*, vol. 12, no. 4, pp. 669–681, Aug. 2005, doi: 10.1109/TDEI.2005.1511092.
[56] H. Jin, T. Andritsch, I. A. Tsekmes, R. Kochetov, P. H. F. Morshuis, and J. J. Smit, "Properties of mineral oil based silica nanofluids," *IEEE Trans. Dielectr. Electr. Insul.*, vol. 21, no. 3, pp. 1100–1108, Jun. 2014.

HOCINE KHELIFA (Member, IEEE) was born in Touggourt, Algeria. He received the bachelor's and Double Diploma (master's and Engineering) degrees in electrical engineering from the National Polytechnic School of Constantine (ENPC), Constantine, Algeria, in 2018, under an arising collaboration with the Ecole Centrale de Lyon, France, where he is currently pursuing the Ph.D. degree in electrical engineering and, more specifically, high voltage engineering. Later, he did the research for two years with the ENPC, and he was involved in synchronous reluctance machine (Syn-RM) and drive and, more precisely, finite element modeling, optimization, and control of this special machine, for a reversible mode of operation. His current research interests include insulation liquid, creeping discharges, and electrostatic charging tendency (ECT) of nanofluids.

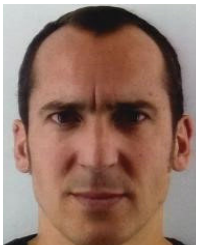

ERIC VAGNON (Member, IEEE) received the French National Teaching Degree ("Agrégation") in electrical engineering from the Université Claude Bernard Lyon 1, in 2005, and the Ph.D. degree from the University Grenoble Alpes, in 2010. As a Research Engineer, he worked in the field of 3D packaging for silicon power devices or the development of liquid metal spreaders for power modules. Since 2016, he has been an Associate Professor at the Ecole Centrale de Lyon and the Ampère Laboratory. He currently works with the Power Electronic Team, Grenoble Electrical Engineering Laboratory (G2Elab). His research interests include high-voltage engineering, dielectric materials characterization, and partial discharge measurement. In addition, as part of the SuperGrid Institute, he defines insulation solutions for medium-frequency transformers and in packaging activities.

ABDERRAHMANE BEROUAL (Fellow, IEEE) was the Head of the High Voltage Group, AMPERE Laboratory, CNRS; a Scientific Expert at the SuperGrid Institute; responsible of the Master Research Program in electrical engineering (2013–2015). He is currently a Distinguished Professor at the Ecole Centrale de Lyon, University of Lyon, France. He is also a Distinguished Visiting Professor of the U.K. Royal Academy of Engineering, Cardiff University, and King Saud University, Saudi Arabia. He supervised more than 45 Ph.D. theses. He is the author/coauthor of more than 500 technical articles, including more than 220 refereed journal articles, five patents, two books, and six book chapters. His main research interests include high-voltage insulation, outdoor insulation, dielectric materials, long air gaps discharge and lightning, modeling of discharges, and composite materials. He is a member of many advisory committees of international conferences, and a Technical Committee of the IEEE CEIDP, UF10 Technical Commission–MT30 of IEC. He was a recipient of the 2016 IEEE T. Dakin Award. He chaired the International Study Group on Streamer Propagation in Liquids of the IEEE–DEIS (1994–1998) and was an Associate Editor of the IEEE TRANSACTIONS ON DIELECTRICS AND ELECTRICAL INSULATION (2018–2020).